9. AERODYNAMIC STABILITY AND CONTROL OF DUCTED-PROPELLER AIRCRAFT

By Ralph L. Maki and Demo J. Giulianetti
Ames Research Center

SUMMARY

Test results from studies of small and large powered models of a dual, tandem, ducted-propeller VTOL design are reviewed, with emphasis on stability and control characteristics through the transition speed range. The characteristics are generally satisfactory. Stability augmentation may be required to reduce Dutch roll tendencies. Further study is needed to evaluate the apparently large side-force gradients in sideslip. Reductions in control effectiveness due to ground proximity are similar to those for tilt-wing V/STOL designs.

INTRODUCTION

A VTOL configuration utilizing tilting ducted propellers in an arrangement such as shown in figures 1 and 2, has powerful hovering control available for pitch and roll by direct modulation of individual propeller thrust. Duct exit vanes operating in the duct slipstream provide yaw control in hover by thrust vectoring. These controls exchange functions in cruising flight. The Bell X-22A VTOL airplane configuration has a similar arrangement.

Investigations of powered models have been made by NASA at small and large scale to study the problems of operation of this concept through the transition speed range. Other studies have indicated reasonable performance for such designs; this discussion is restricted to the stability and control aspects. The studies have provided sufficient data to define the capabilities of the concept and, in general, show it to be quite satisfactory for V/STOL design. Rather than delineate the good features, attention will be directed primarily toward the problems determined in the studies as outlined in figure 3. It appeared likely that control problems in terms of trim requirements, power available, and cross-coupling effects might be anticipated. Possible duct stall and its relation to descent capabilities needed assessment. Effects of ground proximity are also treated.

The large-scale results to be shown in this paper are from tests of a model utilizing 4-foot diameter propellers. These duct units and the drive systems are from the Doak VZ-4DA VTOL airplane which completed its flight research program about 4 years ago. The smaller models tested at Langley Research Center were about 0.3 scale with respect to the large model.

9

NOTATION

a_y lateral acceleration, ft/sec^2

C_D drag coefficient

C_L lift coefficient

C_l rolling-moment coefficient

C_m pitching-moment coefficient

C_n yawing-moment coefficient

C_Y side-force coefficient

D duct exit diameter, ft

g acceleration of gravity, ft/sec^2

HP total input horsepower

h ground height, distance from ground to fuselage under surface, ft

I moment of inertia, $slug\text{-}ft^2$

i_D duct incidence, measured with respect to fuselage reference line, deg

L lift, lb

M_y pitching moment, ft-lb

M_z yawing moment, ft-lb

R_D rate of descent, ft/min

V airspeed, knots

α angle of attack of fuselage reference line, deg

β angle of sideslip, deg

$\triangle$ increment

F   front

R   rear

Y,Z   about the Y or Z axis

α,β derivative of parameter with respect to α or β

$\ddot{\theta}$ pitching angular acceleration, M_y/I_y, rad/sec^2

∞ value out of ground effect

static   value at $V = 0$

DISCUSSION

Transition Characteristics

The transition characteristics of the large-scale model, tested in the Ames full-scale tunnel, and of the smaller model tested at Langley Research Center are plotted in figure 4. Pitching moments, duct angle, and power requirements are given as functions of flight speed for 1-g steady flight. Moments[1] are divided by the inertia representative of a 15,000-lb gross weight airplane to give pitching acceleration values. The small-scale test results show somewhat lower trim duct angles at low speeds; the differences are believed directly relatable to a duct stall phenomenon on the small-scale model to be discussed later. Peak pitching moments occur at 40 to 45 knots for both models, with the small-scale data indicating a peak about 20 percent higher than the large-scale results, and a reduction to zero at a lower flight speed (about 95 knots). Power required is a minimum at about 120 to 130 knots and is roughly half the power required for hover.

Longitudinal Trim and Control

The severity of these pitching-moment variations (fig. 4) in terms of the amount of control required to trim the aircraft are shown in figure 5. Control available and trim requirements are plotted as functions of steady-flight duct angle so that cruise velocities correspond to low duct angles at the left and hover corresponds to a 90° duct angle at the right on this chart. The trim required curve for $\Delta i_D = 0$ is for a center of gravity midway between the front and rear duct rotation axes. Stability about this center of gravity position was approximately neutral, and hence represents a rearmost advisable center of gravity for flight.

---

[1]Model moments were scaled to values for an airplane approximately the size of the Bell X-22A airplane. A scale factor of 0.67 was used for the large model, and 0.20 for the small model.

A boundary of total pitch control available is shown, the left branch displaying the pitch control provided by differential deflection of the duct exit vanes, 20° trailing edge up on the front and 20° down on the rear duct vanes. Vane effectiveness was linear to this deflection for duct angles to 50° or higher. At larger deflections there may be flow separation off the vane, especially for downward vane deflections at high duct angles where the vane protrudes into the free-stream flow. The right branch of the control-available curve bounds the combined effects of differential vanes with differential front-rear propeller thrust. Differential thrust is limited by duct stall for these model tests as thrust was changed by varying propeller rpm; thus, reducing thrust on the forward ducts increases the advance ratio until the inlet lip stalls. (Duct stall will be discussed in more detail later.)

These data show that control power is critical at about 40° duct angle (about 70 knots flight speed) where the margin between the trim requirement and the control available amounts to about 0.4 rad/sec² of pitch acceleration for a 15,000-lb airplane. This represents the control available to handle pitch and roll maneuvering.

The trim requirement can be reduced by deflecting the ducts so that the front duct incidence is less than the rear. The example shown, with the front duct incidence 10° less, about doubles the margin of control for maneuvering in the critical area. Similar gains in control margin can be provided by a moderate forward shift of the center of gravity. Thus, it appears that adequate control for maneuvering can readily be provided.

Descent Rate Limitations

The transition corridor will be limited in one respect for any ducted propeller. As descent rates increase, the advance ratios of the tilted propellers increase until the ducts stall, and the resulting blade stresses or vibration/buffet levels preclude higher rates of descent. In figure 6, curves of required duct angle as functions of flight speed are shown for constant descent rates. Several test boundaries are superposed. In all cases the stall conditions to be described apply to the forward pair of ducts only. The downwash from the front ducts reduces the effective angle of attack at the rear ducts, delaying stall to higher geometric duct angles.

The band labeled "incipient stall" was measured on the large-scale model and represents the earliest measurable indications of stall, generally not discernible by examination of force and moment characteristics. These stall beginnings would be encountered at a descent rate of about 600 ft/min at flight speeds of 55 knots and less. One isolated duct, properly instrumented to monitor blade stresses and vibration, was tested at higher advance ratios to define the boundary at which large stresses and vibrations occurred. This boundary corresponds to those conditions at which flow separation occurs in the duct inlet at the upstream lip (as illustrated in fig. 7), and probably represents the limit rates of descent in flight. High descent rates are possible at flight speeds above 55 knots. At lower speeds, although blade stresses and buffet levels are tolerable, because of the low dynamic pressure, thrust losses accompany the stall; the significance of these losses needs

further study. The incipient stall boundary was used to define the limit for control available from differential thrust (fig. 6); hence, the margins of control available as discussed were conservative. The difference between the incipient and deep lip stall boundaries emphasizes the need for adequate test instrumentation for exploring duct stall phenomena.

The lower boundary in figure 6 was determined in tests of the small-scale models. The outer surface of the duct stalled (see fig. 7) even at zero descent rate. Tests of a large isolated duct of the type used on the small model proved this to be a scale effect. Although the surface pressure distributions on the large duct indicated some degree of separation of the flow over the upper-outer surface, its effects were too slight to be discernible in force or moment data or in model vibration. With a slat installed at the upper leading edge and an enlarged lower lip radius, the small-scale model displayed stall characteristics similar to those measured at large scale.

In summary, then, these data emphasize the care which must be taken in interpreting ducted-propeller data, for various sources and degrees of duct stall phenomena might otherwise lead to erroneous conclusions in predicting flight characteristics.

Lateral-Directional Characteristics

Studies of the lateral-directional characteristics of the ducted-propeller models have revealed several problem areas. The first of these is illustrated in figure 8 where yawing moment as a function of sideslip is shown for three duct incidence settings with the vertical tail both on and off. The vertical-tail volume was sufficient to provide directional stability with the ducts set in the cruise configuration $(i_{D,F} = 5^{\circ}, i_{D,R} = 0^{\circ})$. However, C_{n_β} becomes increasingly unstable at low sideslip angles as duct incidence is increased. At 50° duct incidence, the vertical tail did not measurably change C_{n_β} at low β. Small-scale tests identified an area of flow separation at the tail-fuselage juncture which immersed an increasing tail area with increasing angle of attack. Fences installed near the base of the vertical tail on the large-scale model did not prevent the spread of flow separation. However, tail-fuselage fairings were developed on the small-scale model which alleviated the separation.

There has been general concern about the magnitude of the side force on vehicles with the broad lateral areas of ducted-propeller configurations. It is difficult to assess the magnitude of these side forces. On figure 9 the measured side-force gradients, C_{Y_β}, are ratioed to C_{L_α} in a first attempt to judge the magnitude. This ratio simply relates the side force to a quantity which is very well-defined and understood. The data show that with the ducts set for the cruise condition C_{Y_β} is 30 to 40 percent as large as C_{L_α}, and the ratio increases as duct incidence is increased at transition speeds.

Figure 10 was prepared to assess the results in more meaningful terms - lateral acceleration at various flight speeds. For a 50 ft/sec crosswind gust, and over the flight-speed range for which the ducts will be set in the cruise configuration, increments of about 0.6 to over 1.0 g will be felt. These

magnitudes would be evaluated best by comparison with those for a design with free propellers to determine whether the ducts themselves or the propeller disk area leads to the large side forces. Directly comparable data were not available. Data for a two-propeller STOL model are not representative since the propeller span to the wing-span ratio was relatively small. Some data for a four-propeller model with large wing-tilt angles, that is, in transition configurations, indicate responses of about 1/3 to 1/2 those for the ducted-propeller model. These results, although inconclusive, suggest a problem area peculiar to the ducted-fan design concept.

Free-flight tests of a small-scale model showed Dutch roll oscillations that were unstable at low speeds and still lightly damped at speeds for which 20° duct angle provides trim. Tests were terminated at that point for fear of damaging the model at higher flight speeds. The static data in figure 11 for the large-scale model with ducts set in the cruise configurations suggest that the airplane will have Dutch roll tendencies in cruising flight. The model is directionally stable (as was seen in fig. 8), but the gradient with sideslip is quite low so the model will be lightly damped. The yawing moments are coupled with large rolling moments which are conducive to Dutch roll and hence support the small-scale free-flight findings.

<p align="center">Effects of Ground Proximity</p>

Tests of the effects of ground proximity have been made at both small and large scale. Figure 12 summarizes some of the hover results for $\alpha = 0°$, $\beta = 0°$, and zero roll. Lift and exit-vane control are given as functions of model height above ground. Height is measured to the fuselage undersurface, and is referenced to duct exit diameter. Small-scale data indicate lift increases at low heights and the lift at a height typical for wheel contact is about 20 percent above that with no ground effect. Results from large-scale tests did not include a similar minimum height, but do show that lift increases as the ground is approached.

On the small-scale model exit vanes were deflected differentially on the left and right ducts to control yaw. Losses in control effectiveness were measured at ground heights of less than 2 diameters. At touchdown, the loss is about 40 percent. Tests of the large-scale model at a ground height of about 0.7 diameter showed a loss of pitch control of over 30 percent which is in general agreement with the yaw-control results. Yaw-control tests on a four-propeller tilt-wing model, showing similar control-power losses, are analogous to the ducted-propeller tests since the ailerons used for yaw control operate in the propeller slipstream in a manner similar to the vanes in the duct slipstream.

Figure 13 summarizes the basic longitudinal characteristics of the large-scale model as affected by ground proximity for operation as a STOL or conventional airplane. Lift increases of 10 to 20 percent were measured at the lowest test height. These increases will be beneficial in arresting sink rate during landing flare. Drag reductions will provide additional acceleration on take-off ground roll. Pitching-moment changes mean that the trim requirement

changes with height. However, the magnitude of these moment changes at the low dynamic pressures during a landing approach or climbout after take-off is very small.

CONCLUDING REMARKS

This review of test results on V/STOL models utilizing tilting ducted propellers as combination lift/propulsion/control units may be summarized as follows:

Adequate control is available through the transition speed range. The control margins beyond the trim requirements can be increased through moderate center of gravity shifts and by appropriate configuration conversion techniques.

Duct stall phenomena should not impose undue limitations on the flight envelope.

Directional instability at low flight speeds, and lightly damped stability in cruise may require stability augmentation to reduce Dutch roll tendencies.

Apparently large side-force gradients in sideslip may noticeably reduce passenger comfort in gusty air; this problem needs further study.

Lift increases are measured in proximity to the ground. Large control losses are also encountered which are similar to losses measured for tilt-wing V/STOL designs.

LARGE-SCALE MODEL
THREE-QUARTER REAR VIEW
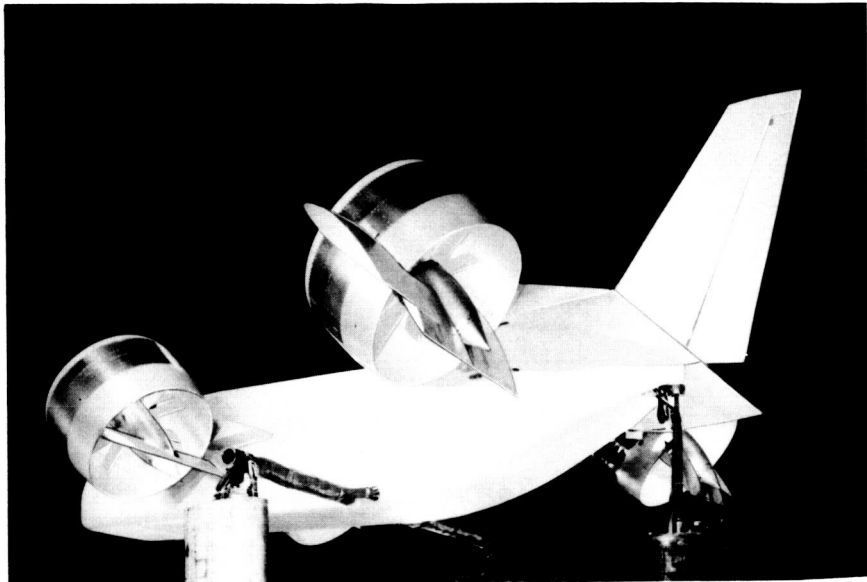
Figure 1   A – 33529.1

LARGE-SCALE MODEL
### OVERHEAD VIEW
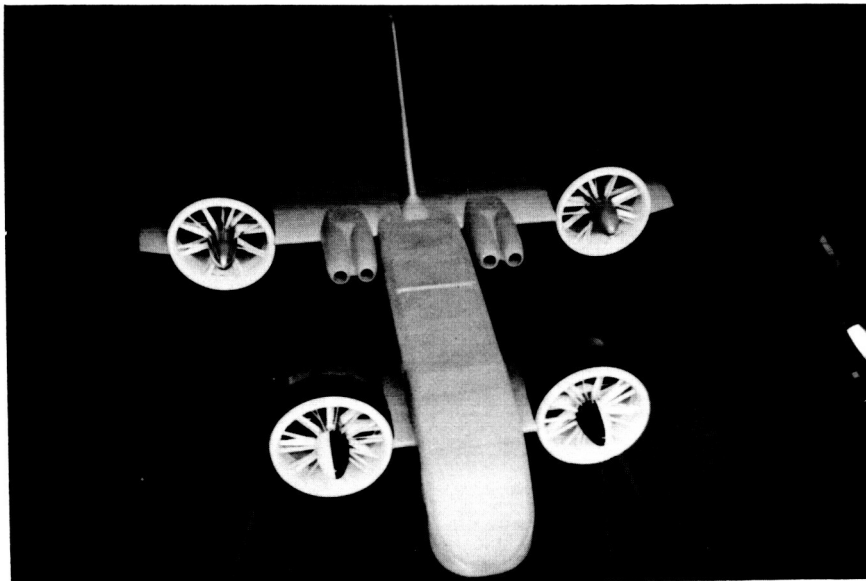
Figure 2   A – 33532

STABILITY AND CONTROL INVESTIGATIONS OF
DUCTED PROPELLER VTOL MODELS

- TRANSITION CHARACTERISTICS

- LONGITUDINAL STUDIES
    - TRIM AND CONTROL
    - DESCENT RATES

- LATERAL-DIRECTIONAL STUDIES
    - DIRECTIONAL STABILITY
    - SIDE FORCE
    - DUTCH ROLL

- GROUND PROXIMITY

Figure 3

TRANSITION CHARACTERISTICS
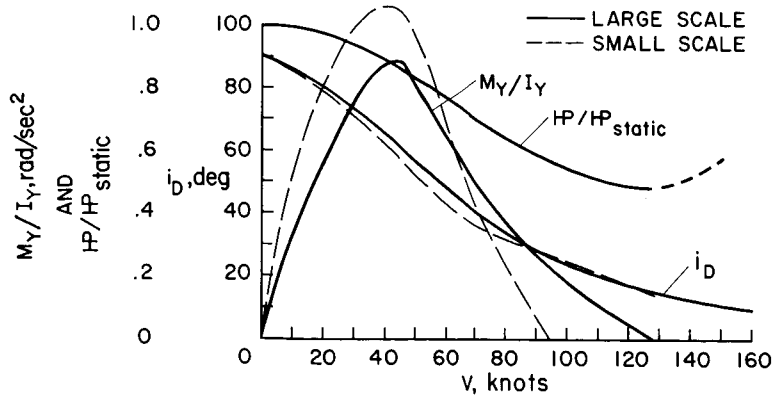
Figure 4

LONGITUDINAL TRIM AND CONTROL
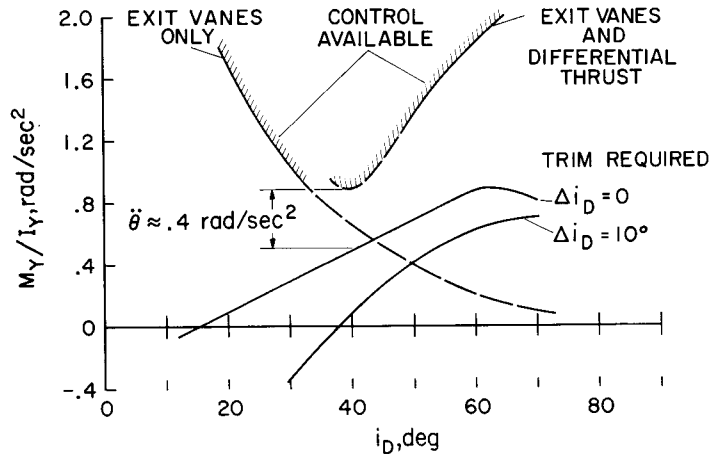
Figure 5

## DESCENT-RATE LIMITATIONS
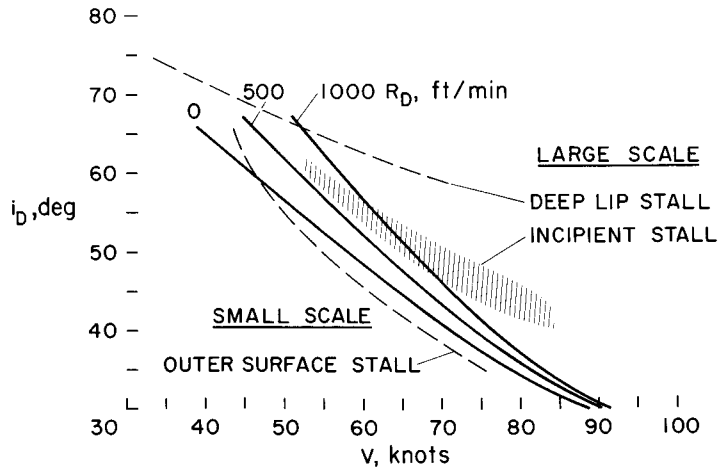
Figure 6

TYPES OF DUCT STALL

OUTER SURFACE
STALL

INLET LIP
STALL
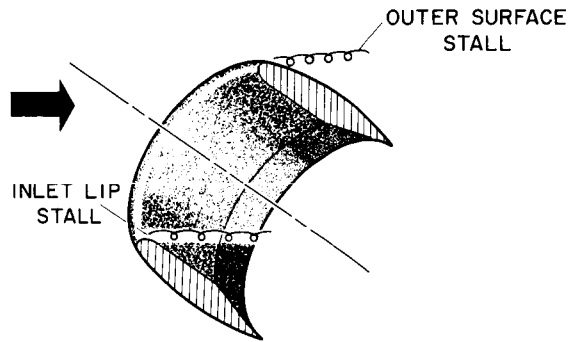
Figure 7

DIRECTIONAL STABILITY
$\alpha = 0°$

TAIL ON

TAIL OFF

CRUISE

$30°$

$i_D = 50°$

C_n

CRUISE

$30°$

$50°$

β, deg

β, deg

Figure 8

125
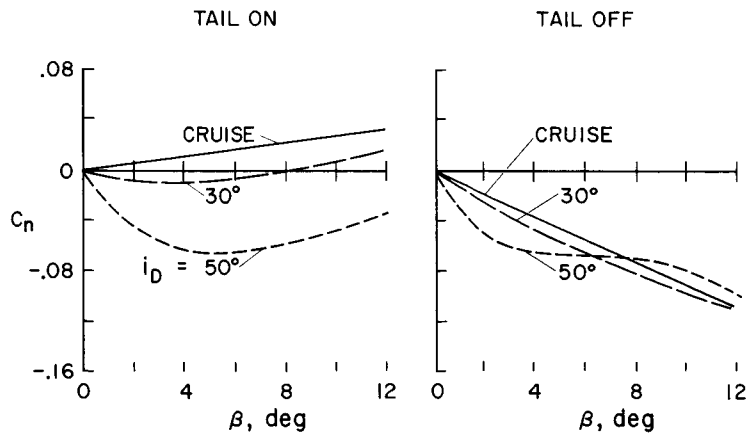
SIDE FORCE – LIFT RELATION
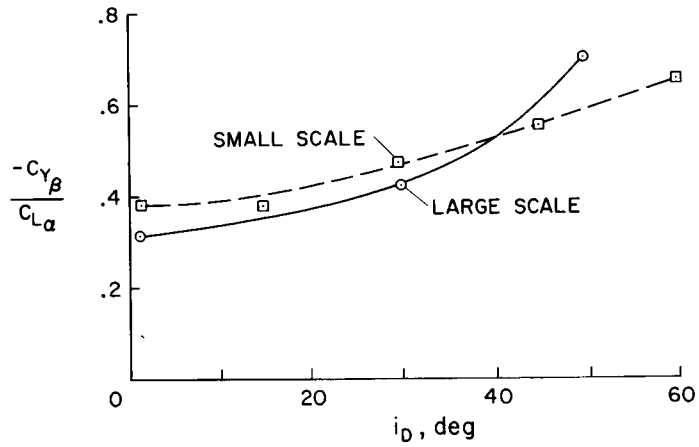
Figure 9

RESPONSE TO CROSSWIND GUST OF 50 FT/SEC
LARGE-SCALE MODELS

Figure 10

126
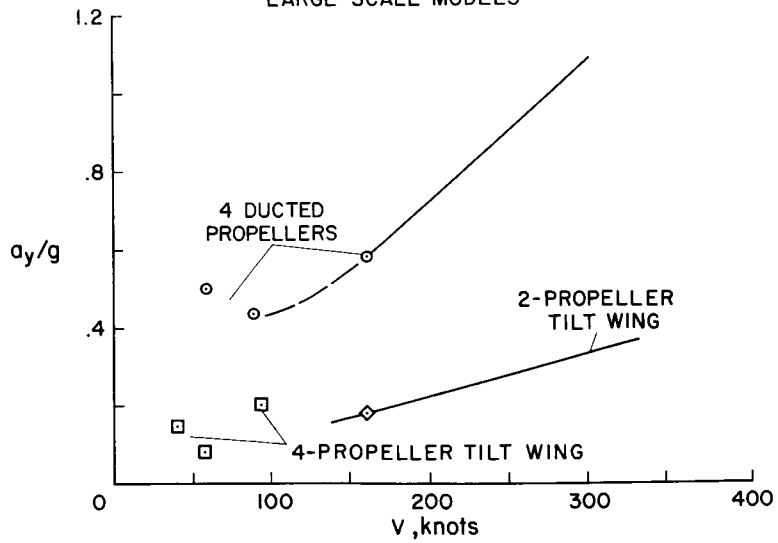
ROLL-YAW COUPLING
CRUISE CONFIGURATION LARGE-SCALE MODEL

c_n

c_l

$\alpha = 8°$ $0°$

β, deg
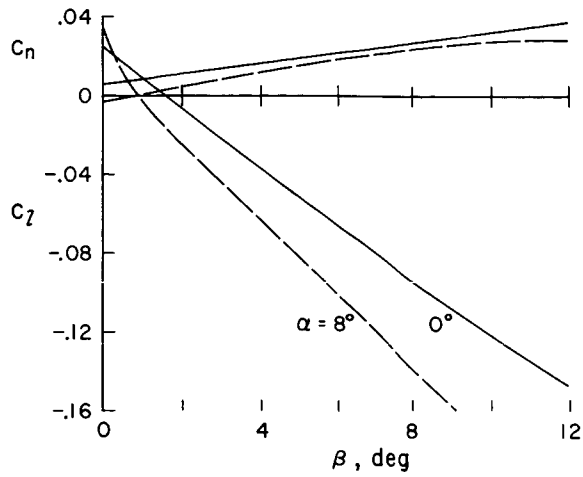
Figure 11

GROUND EFFECTS IN HOVER

L/L_∞

LIFT INCREASE

SMALL SCALE   LARGE SCALE

YAW CONTROL LOSS
SMALL SCALE

TILT-WING VTOL
SMALL SCALE

$M_z/M_{z\infty}$

h/D
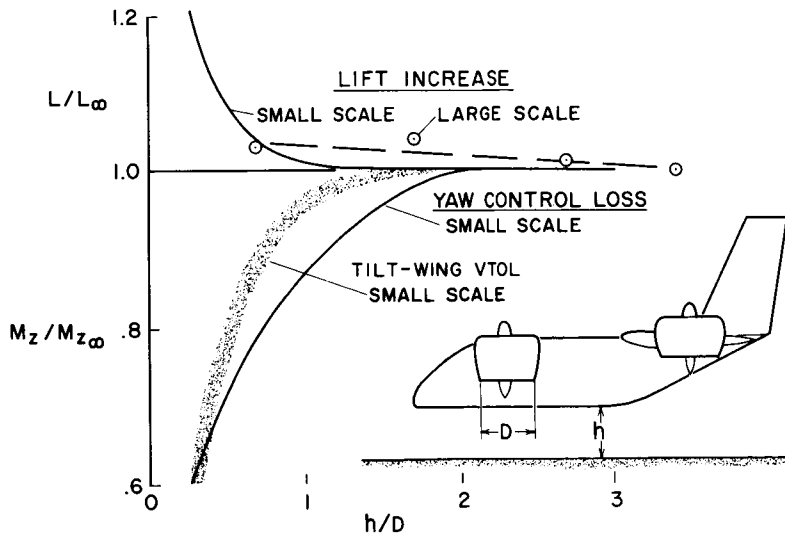
Figure 12

GROUND EFFECTS IN STOL OPERATION
LARGE-SCALE MODEL, $\alpha = 0°$

Figure 13